

The modulating-function waveform analysis method and deep levels in semiconductors

This article has been downloaded from IOPscience. Please scroll down to see the full text article.

1990 J. Phys.: Condens. Matter 2 10359

(<http://iopscience.iop.org/0953-8984/2/51/009>)

View [the table of contents for this issue](#), or go to the [journal homepage](#) for more

Download details:

IP Address: 129.252.86.83

The article was downloaded on 27/05/2010 at 11:21

Please note that [terms and conditions apply](#).

The modulating-function waveform analysis method and deep levels in semiconductors

N C Halder and A A Teate

Department of Physics, University of South Florida, Tampa, FL 33620, USA

Received 30 October 1989, in final form 18 April 1990

Abstract. The modulating-function (MF) waveform analysis method has been generalized and applied to investigate the deep levels in semiconductors. The advantages of the MF method over other available methods—the method of moments, Fourier transform and least-squares—have been discussed and re-emphasized. As examples, the isothermal capacitance transients measured for GaAs (Si implanted) and Si (Au doped) have been analysed. The results for activation energy, capture cross section and density distribution are in general agreement with the experimental and calculated results published earlier.

1. Introduction

In our earlier paper [1] we have described a three-in-one measurement system, i.e. isothermal capacitance transient spectroscopy (ICTS), conductance spectroscopy and capacitance profiling (CP), to study deep levels in semiconductors. The purpose of this paper is to outline a theoretical approach and data analysis program to determine the device (sample) characteristics, such as activation energy, emission rate, capture cross section and trap concentration.

Four different approaches available at present are the method of moments (MM) [2], the Fourier transform (FT) method [3], the least-squares (LS) method [4] and modulating-function (MF) [5] waveform analysis. The MM was first proposed by Kirchner *et al* [6], which was later extended by Ikossi-Anastasiou and Roenker [2]. The MM, which depends on the iteration procedure, requires many iterations and a cut-off correction before achieving a desired accuracy. Furthermore, one has to implement a noise reduction algorithm in the main program. This method, however, is reported to work very well on mainframe computers where time constraint is not a large factor, especially to eliminate the noise and truncation errors. The FT method [3] for deep-level transient spectroscopy (DLTS) study was suggested by Okuyama *et al* [3]. They worked out a procedure for analysing one- and two-trap DLTS signals and emphasized that the peak positions are not necessary in the experimental data. A closer examination of this paper reveals, however, that a very extensive calculation involving fast FT is required to generate real and imaginary parts of the Fourier coefficients. Additionally, if a small amount of noise is present in the measured data, it can give rise to misleading results for the device characteristics, the error could become easily as large as 20–30%. The third method—the LS method—has been advocated by Thurber and Lowney [4] in the study of ICTS obtained with different bias voltages but the same fill voltages. The method is extremely

useful for field effect study of non-exponential transients, which may also arise for several other reasons. With this method, accurate values of activation energy, emission rate and trap concentration have been reported [4] for Pt-doped Si.

In this study we shall follow the MF method, which has recently been introduced [5] but not implemented yet to a significant extent. The MF method is particularly suitable for multiexponential transients, because it has apparently the least noise sensitivity, highest resolution and easy-to-use correction procedure to baseline offset value. It can be adopted, as we shall see later, to smaller computers in the local environment. We have modified the original MF method in three ways.

- (i) We have generalized the MF equations.
- (ii) We have incorporated two distinctly different MFs.
- (iii) We have written a new algorithm to make it work on an AT- or XT-compatible computer.

Finally, we shall demonstrate here its accuracy and efficiency by applying it to the case of ICTS measured from Si (Au doped) and GaAs (Si implanted).

2. Theoretical approach

In this section we discuss the MF method and show how to analyse the experimental data. In the DLTS measurement, one needs [7] a double-box-car integrator to determine the rate window assuming exponential capacitance transients. Here the rate window is kept fixed, but the temperature is varied. One then has to repeat the same operation for another rate window and so on, until the whole range of rate windows is covered. This task is quite time consuming as one has to repeat the same procedure over the same range of temperatures again and again. There is also the possibility of missing some weakly developed DLTS profiles when inappropriate rate windows are selected. These problems do not arise [8] in ICTS measurements as one measures in this case the isothermal transients only once in the entire range of temperatures of interest. One can then easily construct the DLTS signal, if there is any need, from the measured ICTS.

The MF method proposed by Ransom *et al* [5] is specifically geared to ICTS experiments. The capacitance transient due to a single trap level at any temperature T is given by

$$C(t, T) = B + A \exp(-t/\tau) \quad (2.1)$$

where t is the time, τ the time constant, B the baseline constant (offset value) and A the amplitude function. For a multiexponential case, however, it can be rewritten as

$$C(t, T) = B + \sum_i^n A_i \exp(-t/\tau_i) \quad (2.2)$$

and the emission rate

$$(e_n)_i = \tau_i^{-1} = [\sigma_i(T)\langle v_n \rangle N_c / g] \exp(-E_i/kT) \quad (2.3)$$

where E_i is the activation energy of the trap, σ_i the capture cross section, $\langle v_n \rangle$ the average thermal velocity of the carriers, N_c the effective density of states of the conduction band

edge and g the degeneracy factor of the level. The product $\langle v_n \rangle N_c$ can be shown, in the free-electron approximation, to be

$$\langle v_n \rangle N_c = (16m\pi k^2/h^3)T^2 = \gamma_n T^2 \quad (2.4)$$

where

$$\gamma_n = 16m\pi k^2/h^3. \quad (2.5)$$

Therefore,

$$(e_n)_i = a_{ni} T^2 \quad (2.6)$$

with

$$a_{ni} = \sigma_i(T)\gamma_n/g. \quad (2.7)$$

One of the possible forms for capture cross section considered is

$$\sigma_i(T) = \sigma_\infty \exp(-\Delta E_B/kT) \quad (2.8)$$

where ΔE_B is the barrier height energy of the carrier. If the capture cross section is taken to be independent of temperature, a plot of $\ln(T^2/e_n)$ versus T will be linear and, therefore, from the slope of the straight-line plot, one can obtain the values of the activation energy E_i . This is what is generally done in most experimental research work. However, Thurber and Lowney [4] found that an appreciable error could be introduced into the computed value of E_i if $\sigma(T)$ were not properly handled and proposed an alternative practical way of circumventing this problem. This method is somewhat time consuming as it requires additional computations and plotting. We, therefore, suggest another way of using the same original equation but obtain the effective activation energy rather than the simple activation energy:

Let us write equation (2.6) as

$$(e_n)_i = a'_{ni} T^2 \exp(-\Delta E_i/kT) \quad (2.9)$$

where

$$a'_n = \sigma_\infty \gamma_n/g \quad (2.10)$$

and

$$\Delta E_i = E_i + \Delta E_B. \quad (2.11)$$

This ΔE_i , in general, is not as simple as it appears. It will also include the effects of temperature of the energy gap, etc. We now attempt a straight-line fit by plotting $\ln(T^2/e_n)$ versus T . The best value of this slope can be selected for the sample under study. This procedure also enables one to determine experimentally the temperature dependence of $\sigma(T)$ if one can find E_i from another source.

We now return to equation (2.2) and differentiate it to obtain (this procedure eliminates the baseline constant B)

$$\begin{aligned} \dot{C}(t, T) &= (-1)^1 \sum_i^n \frac{A_i}{\tau_i} \exp\left(-\frac{t}{\tau_i}\right) \\ \ddot{C}(t, T) &= (-1)^2 \sum_i^n \frac{A_i}{\tau_i^2} \exp\left(-\frac{t}{\tau_i}\right) \end{aligned} \quad (2.12)$$

etc.

Introducing a MF $\varphi(t)$ and multiplying the above equations by it, one can integrate

$$\int_{T_S}^{T_E} \dot{C}(t, T) \varphi(t) dt = (-1)^1 \sum_i^n \frac{A_i}{\tau_i} \int_{T_S}^{T_E} \exp\left(-\frac{t}{\tau_i}\right) \varphi(t) dt \tag{2.13}$$

where T_E means the end time and T_S the start time of the transient. To obtain the amplitude function A_i , one must satisfy the required condition

$$\dot{C} + \alpha_1 \ddot{C} + \dots + \alpha_m \overset{(m+1)}{C} = 0 \tag{2.14}$$

where the coefficients α_m are written for convenience to fulfil the condition

$$\overset{(m)}{\tau} - \alpha_1 \overset{(m-1)}{\tau} + \dots + (-1)^m \tau = 0. \tag{2.15}$$

The MF is normalized to zero over the entire transient time:

$$\left[\overset{(m)}{\varphi(t)} \right]_{T_S} = \left[\overset{(m)}{\varphi(t)} \right]_{T_E} = 0. \tag{2.16}$$

Thus the above equations lead to

$$\int_{T_S}^{T_E} \dot{C}\varphi(t) dt + \alpha_1 \int_{T_S}^{T_E} \ddot{C}\varphi(t) dt + \dots + \alpha_n \int_{T_S}^{T_E} \overset{(m+1)}{C} \varphi(t) dt = 0. \tag{2.17}$$

It can be reduced from a C -differential to a $\varphi(t)$ -differential equation easily by partial integration:

$$\int_{T_S}^{T_E} \dot{C}\varphi(t) dt - \alpha_1 \int_{T_S}^{T_E} \dot{C}\dot{\varphi}(t) dt + \dots + (-1)^m \alpha_m \int_{T_S}^{T_E} \overset{(m+1)}{C} \varphi(t) dt = 0 \tag{2.18}$$

Let us consider MFs of the form UV . Then the product derivative rule gives

$$\overset{(m)}{\varphi(t)} = \sum \overset{(m)}{(j)} \overset{(m-j)(j)}{U} V. \tag{2.19}$$

We choose two different types of function to test the convergency of the above results.

For MF 1,

$$\varphi(t) = (t - T_S)^{P_1} (T_E - t)^{P_2}. \tag{2.20}$$

We find the m th derivatives:

$$U = [P_1! / (P_1 - m)!] (t - T_S)^{P_1 - m} \tag{2.21}$$

and

$$V = (-1)^m [P_2! / (P_2 - m)!] (T_E - t)^{P_2 - m}.$$

For MF 2,

$$\varphi(t) = \{\sin[a(t - T_S)]\}^P. \tag{2.22}$$

We substitute

$$a = l\pi / (T_E - T_S) \tag{2.23}$$

and

$$x = t - T_s.$$

Then

$$\begin{aligned} \sin^P(ax) &= (1/2i)^P [\exp(iax) - \exp(-iax)]^P \\ &= (1/2i)^P \sum_{R=0}^P \binom{P}{R} [-\exp(-ax)]^R [\exp(iax)]^{P-R}. \end{aligned} \quad (2.24)$$

Now using the product rule it is easily seen that

$$\varphi = \frac{i^{m-P}}{2^P} \sum_{R=0}^P \binom{P}{R} (-1)^R (P-2R)^m \exp[ia(t-T_s)(P-2R)]. \quad (2.25)$$

The above two MFs have been selected in rather general form. One can find reasonably good answers, as will be seen later, with $P = 1$ or 2 . The value of n depends on the number of defect levels present, usually $n = 1$ or 2 . An analysis of the experimental data with either of these two MFs should lead to the same order of accuracy in the measured ICTS plots if no error is present in the computation and/or inappropriate truncation error is made in the integration procedure. In the following section we implement this approach, demonstrating its accuracy and efficiency.

3. Experimental and operational procedure

We are now ready to apply the MF method just illustrated to the case of Si (Au doped) and GaAs (Si implanted). These two materials have been studied previously [9–15] and their important deep levels have been identified. These samples are actually Schottky diodes and mounted on TO-5 headers. The Si sample was obtained from the National Institute of Standard and Technology (sample NBS2) and the other from the Wright-Patterson Air Force Base (sample GAS2).

Sample NBS2, with the laboratory code number Au76N10.8, was prepared from 5–10 Ω cm on (111) n-type Si. The B diffusion had a surface concentration of about 10^{18} cm^{-3} and a junction depth of about 2 μm . Au was diffused into the diode from the back side at about 800 $^\circ\text{C}$ for 24 h. Sample GAS2 was actually prepared by Sumitomo Company with the laboratory code 604641-019 # B2. This is a liquid-encapsulated Czochralski sample with Si implantation. The donor concentration N_d was about 5.62×10^{16} cm^{-3} and the barrier height φ_B about 0.821 V. The other details—influence, surface concentration, etc—are not available.

The experimental set-up used for this investigation is scanning DLTS (SDLTS), which has already been described previously. We measured the ICTS transients at a frequency of 1 MHz in the temperature range 100–380 K. The transients were recorded by highly automated, self-controlled and powerful software DLTS.PRG at 2 K intervals, a bias voltage from -3 to -10 V, positive pulsing to a maximum of 0 V and a pulse hold time from 0.001 to 1 s. The main program DLTS.PRG is made up of several auxiliary programs and two correction programs, CAB.CORR and CLIP.CORR. The program CAB.CORR is needed to correct for the inherent cable capacitance together with the terminals. The fluctuation of the line voltage and other electrical noise introduced in the measuring signal was suppressed by the CLIP.CORR and HP-16083A placed in the electrical circuit.

Together with this data acquisition, simultaneous plottings were done with two programs, PLOT CV and PLOT CT. The first program, PLOT CV, enables one to plot all C–V data obtained from CP. There are two options available to the user: to plot on the screen,

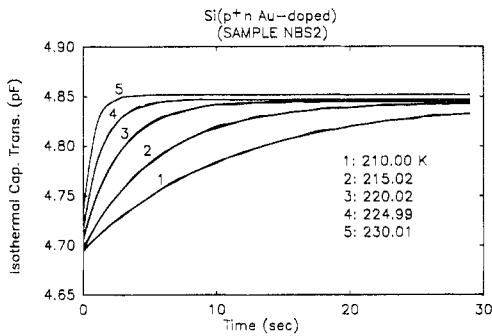


Figure 1. Measured and calculated plots of the capacitance transients for Si (Au-doped p⁺-n) (sample NBS2). The calculated plots are shown by broken lines which in most part overlap the measured plots.

or to plot on the HP plotter. Furthermore, plotting of hard copies can be accomplished by the use of either AGPLOT or SIGMAPLOT. It is convenient to use AGPLOT which is rather quick and tailored to the experiment.

The second plotting program, PLOTCT, is specifically designed for C-T data from DLTS.PRG. It can make one to six plots depending upon one's desire. Like PLOTCTV, PLOTCT can be used for viewing plots on either the screen or hard copies through the HP plotter. It should be noted that these two programs assume that the plotting files are already saved.

After the experiment is completed, the user is directed to the calculation programs stored in directory CTPLT.CAL. There are four programs available in this directory: CON2, DSP14, ECD4 and DATE4. The purpose of the first program, CON2, is to change the format of the transient data file, SAMPLE1.DAT, to another format depending upon the need of the user. This program does not perform any calculation, but it generates two files, SAMPLE1.DAF and SAMPLE1.DAS, to be used later.

The second program, DATE4, is a very useful program as it can produce the DLTS spectra from the transient data measured by DLTS.PRG program. Should there be any need to view the DLTS spectra, one could resort to this program with the help of data already stored in SAMPLE1.DAF file. This program also calculates the interface state density distribution as a function of temperature.

The third program, DSP14, first reads in the transients from the original data file SAMPLE1.DAT and calls a subroutine to attempt a multiexponential fit to the old transients and generates a file SAMPLE1.RXX.

The fourth program, ECD4, calculates all the final results from data file SAMPLE1.RXX. It first constructs the Arrhenius plots effective using a LS fitting routine. The values of the activation energy, emission rate and capture cross section can be obtained from the linearity of the $\ln(T^2/e_n)$ versus $1/kT$ plots.

4. Results and discussion

4.1. Amplitude functions and time constants

In figure 1, we illustrate the measured and calculated results of the transients for one of the samples (NBS2). These calculations refer to one exponential function and MF 1. The measured and calculated values match remarkably well. We have tried this comparison at other temperatures also and found the fitting extremely good, well within 0.05% error. Sample GAS2 showed no difference. Attempts to fit the experimental data were made with all combinations possible:

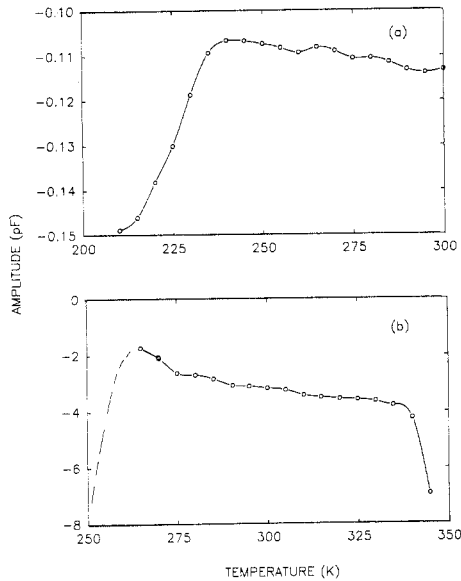


Figure 2. The plots of the amplitude functions A : (a) Si; (b) GaAs.

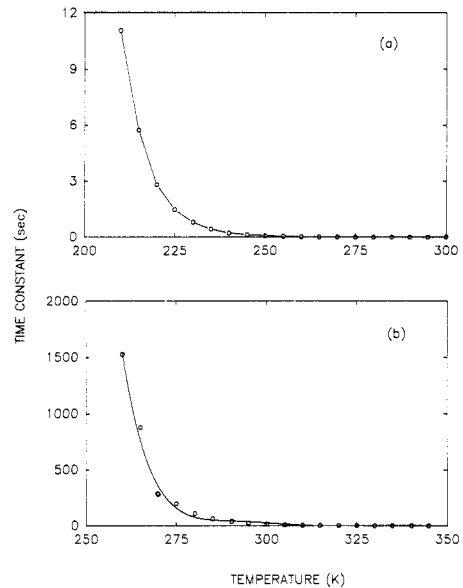


Figure 3. The plots of the time constants τ : (a) Si; (b) GaAs.

- (i) one exponential function and MF 1;
- (ii) two exponential functions and MF 1;
- (iii) one exponential function and MF 2;
- (iv) two exponential functions and MF 2.

In the present investigation, only combinations (i) and (ii) worked well; the others gave much larger errors and wider deviations from linearity in the Arrhenius plots to be discussed later.

One way to assess the goodness of the fit of the transients is to look at the amplitude functions displayed in figure 2. These are characterized by the time constants and the nature of the MF selected in the analysis (in this case MF 1). The time constant plots are shown in figure 3. The modulations in the amplitude functions indicate some general trend; its features strongly reflect the features of the ICTS transients. The time constant plots follow the usual trend of $[\exp(E/kT)]/T^2$. For sample GAS2, in the region of low temperatures (below 250 K), the time constant is many times larger than that for sample NBS2. This is due to the much larger value of the series capacitance for GaAs (142.4 pF at 260 K) than for Si (6.3 pF at 210 K).

4.2. Carrier concentration and depth profiles

For the determination of concentration–depth profiles, we have made C–V measurements assuming that the device capacitance is in a parallel configuration with the resistance. These results are shown in figure 4. For the Si sample we have not probed deep enough with a lower voltage (stopped at -5 V). Furthermore, doping in this sample was done by thermal diffusion contrary to ion implantation in the GaAs sample. The carrier concentration in the two samples are about 10^{15} cm^{-3} and 10^{16} cm^{-3} , respectively. The effect of thermal distribution of the carrier concentration is significant; one such example is included in figure 4(b) for GaAs. For the ICTS measurement, these data are

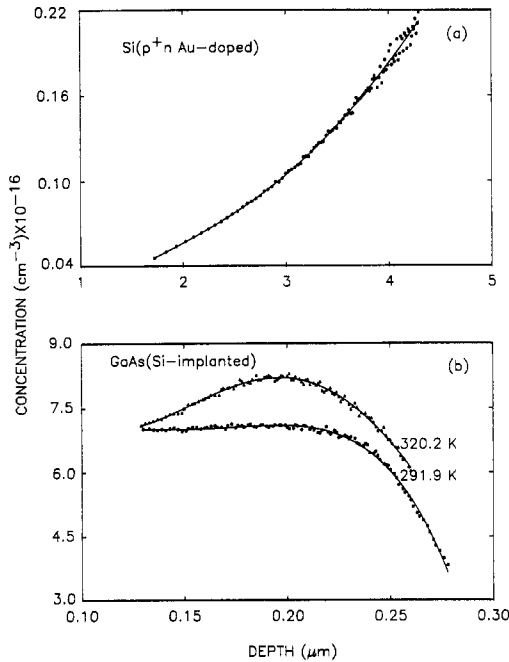


Figure 4. The concentration–depth profiles: (a) Si; (b) GaAs.

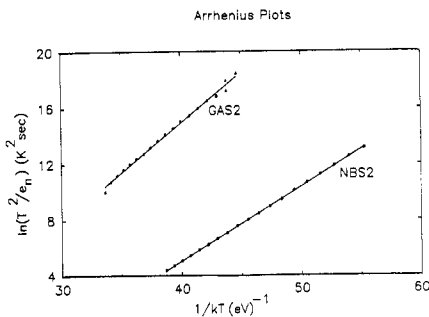


Figure 5. Arrhenius plots for the two samples: (a) Si; (b) GaAs.

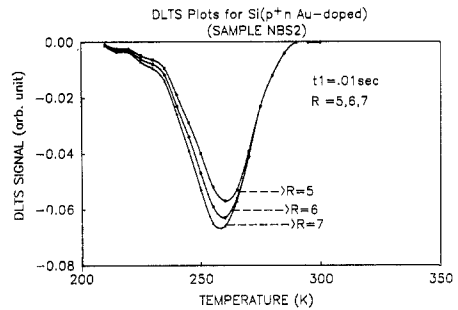


Figure 6. DLTS plots for Si (Au-doped p+n) (sample NBS2) at various rate windows *R*.

very helpful as one needs to know the linear part of the concentration–depth profile to establish the input parameters for completely populating and depopulating the trap levels.

4.3. Arrhenius plots and device characteristics

The Arrhenius plots corresponding to equation (2.9) are displayed in figure 5. As mentioned before, the experimental data were fed through the program DSP14 assuming only one trap level in each case (in this case the EL2 level for GaAs and a deep acceptor

Table 1. Summary of data for GaAs (Si implanted).

| ΔE_i (eV) | σ (cm ²) | Reference |
|----------------------|--------------------------------|-----------|
| 0.78 | 5×10^{-14} | [14] |
| 0.81 | 15 | [15] |
| 0.82 | 2 | [13] |
| 0.83 | 1.2 | [12] |

Table 2. Summary of data for Si (Au doped).

| ΔE_i (eV) | Level | Reference |
|------------------------|-------|-----------|
| 0.33 ± 0.03 | d | [9] |
| $(0.53-0.57) \pm 0.03$ | a | [11] |
| $(0.32-0.34) \pm 0.03$ | d | [11] |
| 0.34 | d | [10] |
| 0.54 | a | [10] |

Table 3. Device characteristics (present work).

| Sample | σ_x (cm ²) | γ_n (m ⁻² s ⁻¹ K ⁻²) | ΔE_i (eV) |
|--------|----------------------------------|--|----------------------|
| Si | 3.412×10^{-15} | 3.001×10^{25} | 0.530 |
| GaAs | 1.5×10^{-15} | 3.001×10^{25} | 0.753 |

level for Si). A LS fitting program gave perfect linearities in both cases. Departures from linearity would occur for samples with two or three exponential components (defect levels), which apparently are not the case here. The final results obtained for the two devices are given in tables 1–3.

4.4. DLTS signals and distribution functions

The DLTS signals were recovered from the ICTS plots using

$$S(T) = [C(t_1, T) - C(t_2, T)]/\Delta C_0 \quad (4.1)$$

for fixed rate windows

$$R = t_2/t_1 \quad (4.2)$$

where

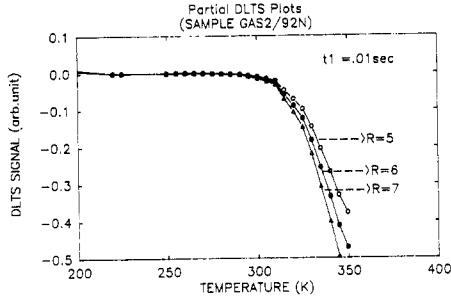


Figure 7. Partial DLTS plots for GaAs (sample GAS2) at various rate windows R .

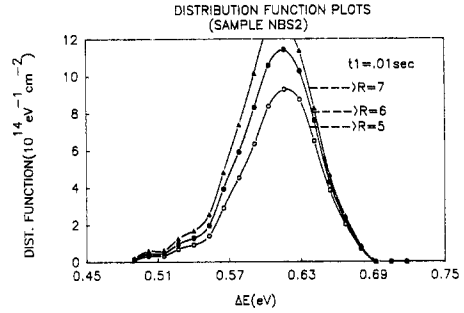


Figure 8. Plots of the interface density distribution function for Si (sample NBS2).

$$\Delta C_0 = C(0) - C(\infty). \quad (4.3)$$

For three R -values of 5, 6 and 7 and $t_1 = 0.01$ s, $S(T)$ plots are shown in figures 6 and 7. Only partial DLTS signals are shown for sample GAS2. A complete profile of the DLTS signal is not necessary for the Arrhenius plot drawn in figure 5(b). However, for the time constant, one usually gives the value with reference to the peak maximum or minimum:

$$\tau_{\max/\min} = (t_2 - t_1)/\ln(t_2/t_1). \quad (4.4)$$

Although higher values of R moves the peak minimum slightly to the left (smaller temperature), it is rather insensitive to the determination of other parameters such as activation energy and capture cross section.

We have finally calculated the defect density distribution. According to Zhang *et al* [16], it is given by

$$N_{ss}(E_{\max}) = [N_d \varepsilon / C(t_1)^2] \{1/[kT \ln(t_2/t_1)]\} \Delta C(t_2, t_1) \quad (4.5)$$

where N_d is the donor concentration, ε the dielectric constant and

$$E_{\max} = E_c - kT \ln[\sigma_z \langle v_n \rangle N_c (t_2 - t_1) / \ln(t_2/t_1)] \quad (4.6)$$

or

$$\Delta E = E_c - E_{\max} = kT \ln[\sigma_z \langle v_n \rangle N_c (t_2 - t_1) / \ln(t_2/t_1)]. \quad (4.7)$$

The program DATE4, as outlined before, gives the distribution plots from the experimental DLTS signals. We show in figure 8 the plots for sample NBS2.

5. Summary and conclusions

In this paper we have presented a theoretical and computational procedure to investigate the measured ICTS by the SDLTS system already proposed earlier [1]. The entire program is centred around an AT-compatible Zenith-248 computer of 10 MHz speed at the actual experimental site. A typical experiment with four-sample probe will require about a day (6–8 h) for completion, including all data acquisition, analysis and plotting. During the course of the experiment and data analysis, one can view and monitor every single step

on the screen as the experiment and/or data analysis progress. This is done purposely, so that one could discontinue momentarily or totally should there be any need.

We first consider the results obtained for sample NBS2, which actually is a $p^+ - n$ junction diode. The main DLTS peak in this sample appears to be a majority carrier peak due to an Au acceptor level. Our measured values, as given in table 3, are $\Delta E_i = 0.530$ eV and $\sigma_\infty = 3.412 \times 10^{-15}$ cm². These two values are in excellent agreement with the values $\Delta E_1 = 0.53 - 0.57$ eV summarized in table 2. The donor level peak, which has been detected by several workers [9–11], also appeared at $E_i = 0.33$ eV (see figure 6) at around 200 K. However, because this peak was very weak (about 15 times smaller than the main peak), we have not analysed it any further. The trap density $N_T = 2(\Delta C/C)N_s$, where N_s is the shallow dopant density in the sample, was not determined as N_s was not known with certainty. We find, however, a calculation of N_{ss} (i.e. ISD) from equation (4.5) gives a reasonable N_{ss} -value of about 1.3×10^{15} eV⁻¹ cm⁻², when $N_d = 10^{18}$ cm⁻³ is used. There is an assumption made in this calculation. Normally, the interface states and bulk states exist side by side in the Schottky barrier region. For the interface states, the peak position and peak temperature are sensitive to the applied pulse voltage (i.e. they are field dependent), but for the bulk states these are field independent. This point has been verified for MOS and MIS structures by Yamasaki *et al* [17]. The plots displayed in figure 8 depict more or less the DLTS peak shape in reverse order.

Sample GAS2, which is GaAs with a Si implantation, also shows a majority-carrier peak. From our measurement, we find the effective value of the activation energy ΔE_i to be 0.711 eV and the capture cross section σ_∞ to be 2.45×10^{-16} cm². This value of ΔE_i is found to be somewhat smaller than the values reported earlier for similar samples. Some of the recently published [12–15] values on this sample are also summarized in table 1. We then measured a few more similar samples (GAS3, GAS4, etc). In these latter samples, the value of the activation energy ΔE_i turned out to be about 0.75 eV, which agrees very well with the value of 0.78 eV reported by Kitagawa *et al* [14]. It should be mentioned here that for GaAs (doped or implanted) this value could range from 0.72 to 0.82 eV depending upon the concentration and nature of the dopant. It is quite conceivable that sample GAS2 might be contaminated with some impurity, possibly Cr. We are at present pursuing an investigation into this possibility.

References

- [1] Halder N C and Bisbee J E 1990 unpublished
- [2] Ikossi-Anastasiou K and Reonker K P 1986 *J. Appl. Phys.* **61** 182
- [3] Okuyama M, Takamura H and Hamakawa Y 1983 *Solid-State Electron.* **26** 689
- [4] Thurber W R and Lowney J R 1987 *J. Appl. Phys.* **62** 534
- [5] Ransom C M, Chappel T I, Freeouf J L and Kirchner P D 1986 *Proc. Symp. on Material Characterization, (Palo Alto, CA, 15–17 April 1986)* (Pittsburgh, PA: Materials Research Society) pp 337–42
- [6] Kirchner P D, Schaff W J, Maracas G N, Eastman L F, Chappel T I and Ransom C M 1981 *J. Appl. Phys.* **52** 6462
- [7] Lang D V 1974 *J. Appl. Phys.* **45** 3023
- [8] Thurber W R, Forman R A and Phillips W A 1982 *J. Appl. Phys.* **53** 7397
- [9] Day D S, Tsai M Y, Streetman B A and Lang D V 1979 *J. Appl. Phys.* **50** 5093
- [10] Stolt L and Bohlin K 1985 *Solid-State Electron.* **28** 1215
- [11] Thurber W R 2 January 1986 Informal DLTS Round Robin on Au-doped Si (*National Institute of Standards and Technology, MD*), Report
- [12] Bhattacharya P K, Rhee J K and Owen S J T 1981 *J. Appl. Phys.* **52** 7224
- [13] Dhar S, Seo K S and Bhattacharya P K 1985 *J. Appl. Phys.* **58** 4216
- [14] Kitagawa A, Usami A and Wada T 1988 *J. Appl. Phys.* **63** 414

- [15] Katayama M, Usami A and Wada T 1987 *J. Appl. Phys.* **62** 528
- [16] Zhang H, Aoyagi Y, Iwai S and Namba S 1987 *Appl. Phys. Lett.* **50** 341
- [17] Yamasaki K, Yoshida M and Sugano T 1979 *Japan. J. Appl. Phys.* **18** 113